

Supporting Information

Highly selective carbon dioxide adsorption in a water-stable
Indium-organic framework material

Jin-Jie Qian,^{a,b*i*} Fei-Long Jiang,^a Da-Qiang Yuan,^a Ming-Yan Wu,^a Shu-Quan
Zhang,^{a,b} Lin-Jie Zhang,^{a,b} Mao-Chun Hong*^a

^aState Key Laboratory of Structure Chemistry, Fujian Institute of Research on the
Structure of Matter, Chinese Academy of Sciences, Fuzhou, Fujian, 350002, China

^bGraduate School of the Chinese Academy of Sciences, Beijing, 100049, China

*To whom correspondence should be addressed: E-mail:hmc@fjirsm.ac.cn; Fax:
+86-591-83794946; Tel: +86-591-83792460

Table of Contents

Section S1. Experimental Procedures	S2-S3
Section S 2. X-ray Crystal Structure	S4-S5
Section S 3. Powder X-Ray Diffraction	S6
Section S 4. TGA Plots	S6
Section S 5. Heat of Adsorption	S7-S8
Section S 6. IAST Selectivity	S9-S11
Section S7. Comparisons of CO₂ uptake capacities and selectivities of CO₂ over CH₄	S12-S13
Section S8. References	S14-S15

1. Experimental Procedures

1.1 Materials and Methods. All the syntheses were performed in 25 mL glass vial under autogenous pressure. All reactants are reagent grade and used as purchased commercially without further purification. The power X-ray diffraction patterns were collected by a Rigaku DMAX2500 X-ray diffractometer using Cu K α radiation ($\lambda=0.154$ nm). Gas adsorption measurement was performed in the ASAP (Accelerated Surface Area and Porosimetry) 2020 System. Elemental analyses for C, H, N were carried out on a German Elementary Vario EL III instrument.

1.2 Synthesis of [In₂(OH)₂(BPTC)]•6H₂O (InOF-1). A mixture of In(NO₃)₃•5H₂O (0.40 mmol, 156 mg) and H₄bptc (0.10 mmol, 33 mg) in N,N'-dimethylformamide (DMF) (5 ml) and CH₃CN (5 ml) with an additional 0.2 ml HNO₃ (65 wt %) was placed in a 25ml vial, which was heated at 85 $^{\circ}$ C for 3 days, and cooled to room-temperature. After washed by fresh DMF, the colorless crystals **InOF-1** were obtained in *ca.* 72% yield (90 mg) based on In(NO₃)₃•5H₂O. Elemental analysis was calculated for activated C₄O_{2.5}H₂In_{0.5} (Mr = 147.47): C, 32.58%; H, 1.37%. Found: C, 36.08%; H, 1.57%. The phase purity of the sample was confirmed by powder X-ray diffraction (PXRD).

1.3 X-ray Crystallography. The fraction data was collected on a Rigaku Mercury CCD diffractometer equipped with a graphite-monochromated Mo K α radiation ($\lambda=0.71073\text{\AA}$) at room temperature and the structure was resolved by the direct method and refined by full-matrix least-squares fitting on F^2 by SHELX-97.¹. The hydrogen atoms of the water molecules were found in the electron density map

and refined by riding. Crystallographic data and structure refinement parameters for **InOF-1** are listed in Table S1. We employed PLATON/SQUEEZE² to calculate the contribution to the diffraction from the solvent region and thereby produced a set of solvent-free diffraction intensities. The final formula was calculated from the SQUEEZE² results combined with elemental analysis data and TGA data. More details on the crystallographic studies as well as atomic displacement parameters are given in Supporting Information as CIF files. Crystallographic data for the structures reported in this paper have been deposited in the Cambridge Crystallographic Data Center with CCDC reference number 890421 for **InOF-1**.

Table S1. Crystal Data and Structure Refinement for **InOF-1**.

complex reference	InOF-1
chemical formula	C ₈ H ₉ InO _{7.5}
formula mass	169.99
crystal system	Cubic
space group	<i>I</i> 4 ₁ 22 (#. 98)
<i>a</i> (Å)	15.5665(6)
<i>b</i> (Å)	15.5665(6)
<i>c</i> (Å)	12.322(1)
α (°)	90.00
β (°)	90.00
γ (°)	90.00
unit cell volume	2985.4 (4)
temperature (K)	293(2)
<i>Z</i>	8
F(000)	1328
no. of reflections measured	11697
no. of independent reflections	1687
R _{int}	0.0240
final R1 values (I>2σ(I))	0.0160
final wR (F ²) values (I>2σ(I))	0.0480
goodness of fit on F ²	1.175
flack parameter	0.26(4)

2. X-ray Crystal Structure.

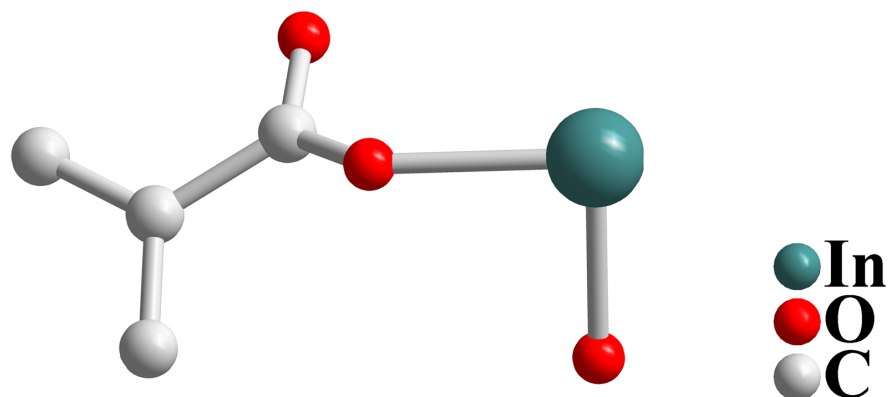


Figure S1. Asymmetric unit of **InOF-1** (hydrogen atoms have been omitted for clarity).

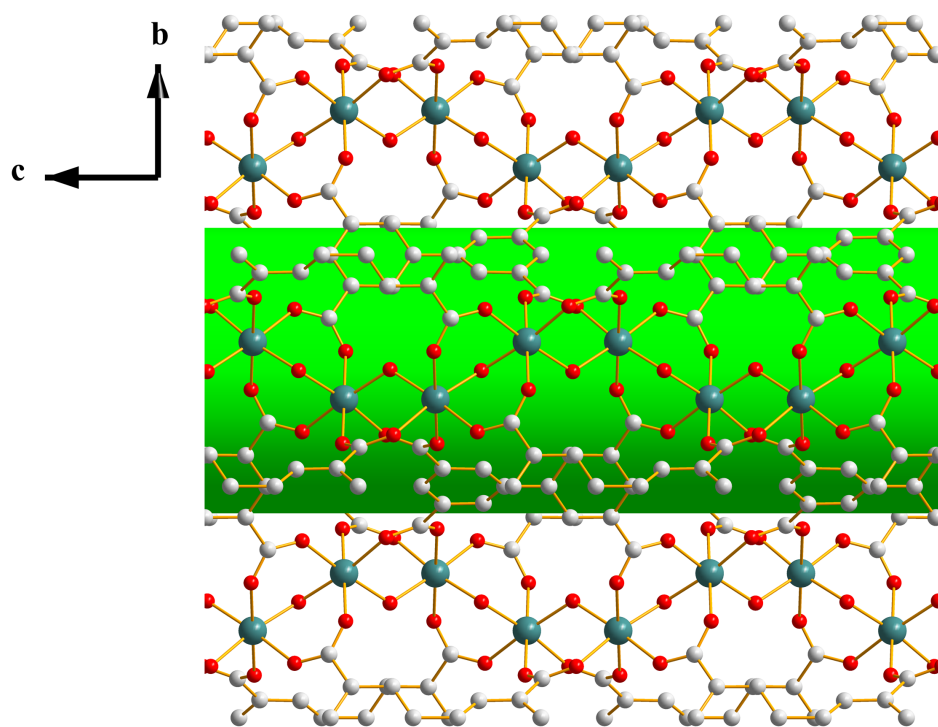


Figure S2. Viewd along the α axis for **InOF-1**.

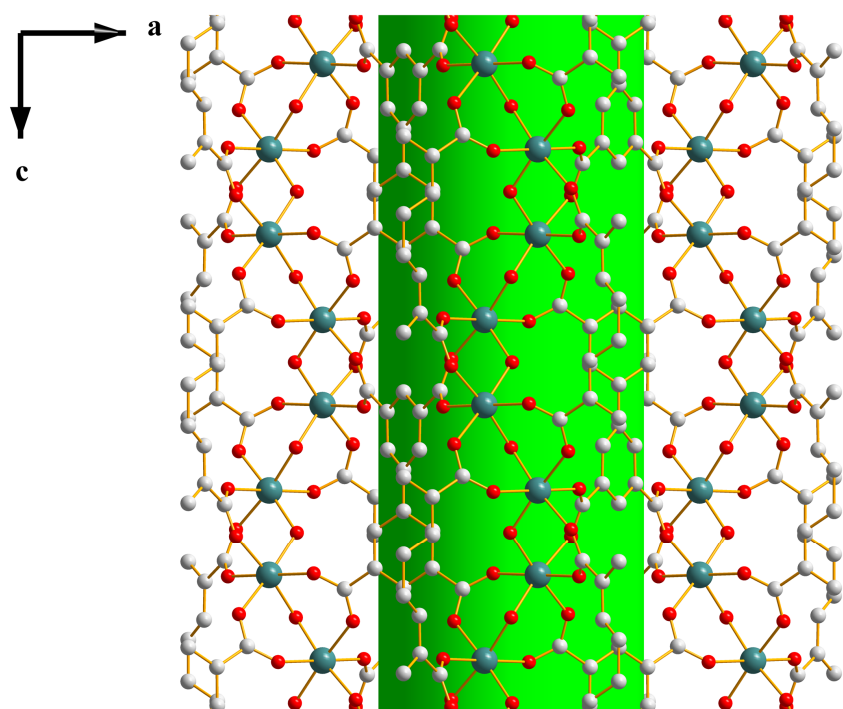


Figure S3. Viewd along the *b* axis for **InOF-1**.

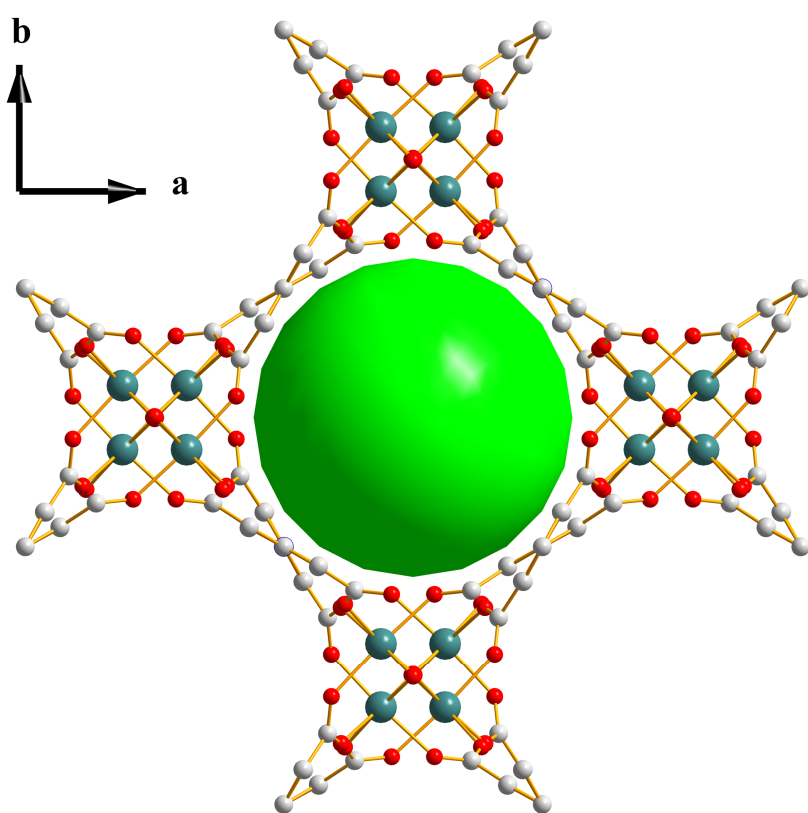


Figure S4. Viewd along the *c* axis for **InOF-1**.

3. Powder X-Ray Diffraction

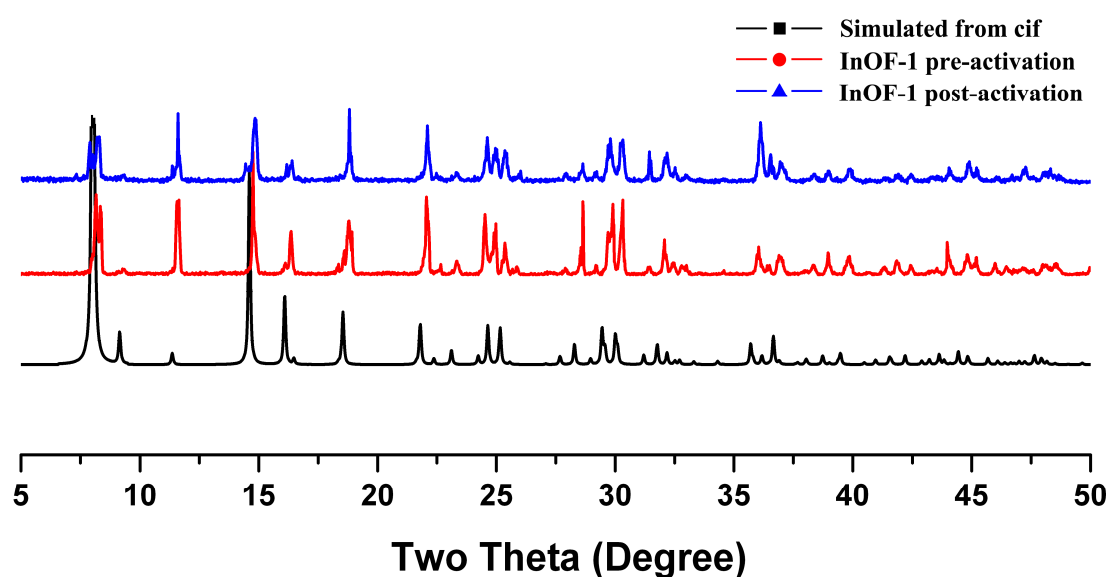


Figure S5. Pre-activation and post-activation experimental and simulated PXRD for **InOF-1** indicating the phase purity of the as-synthesized product.

4. TGA Plots for InOF-1

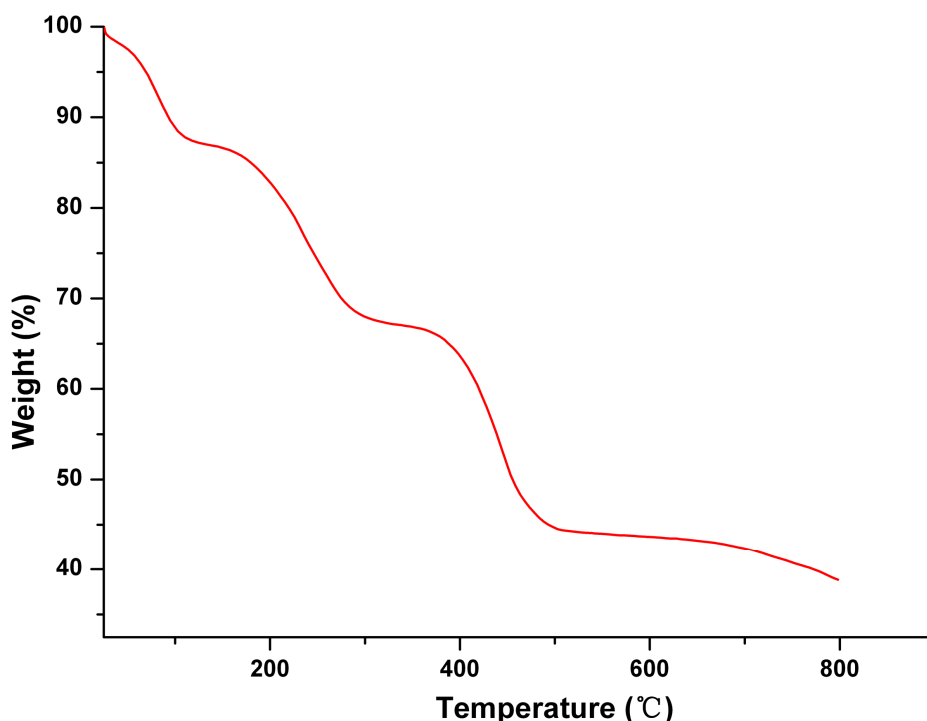


Figure S6. Thermal gravimetric analysis (TGA) for **InOF-1**.

5. Heat of Adsorption (kJ mol^{-1})

CO_2 and CH_4 isotherms measured at 273 K and 296 K for **InOF-1** were fit to the following Equation 1.³

The adsorption isostere is represented by

$$\ln \left(\frac{P}{P_0} \right) = q_i / RT + C \quad (1)$$

where

q_i = isosteric heat of adsorption

C = unknown constant

The isosteric heat of adsorption, q_i is determined by finding the slope of $\ln (P/P_0)$ as a function of $1/RT$ for a set of isotherms measured at different temperatures.

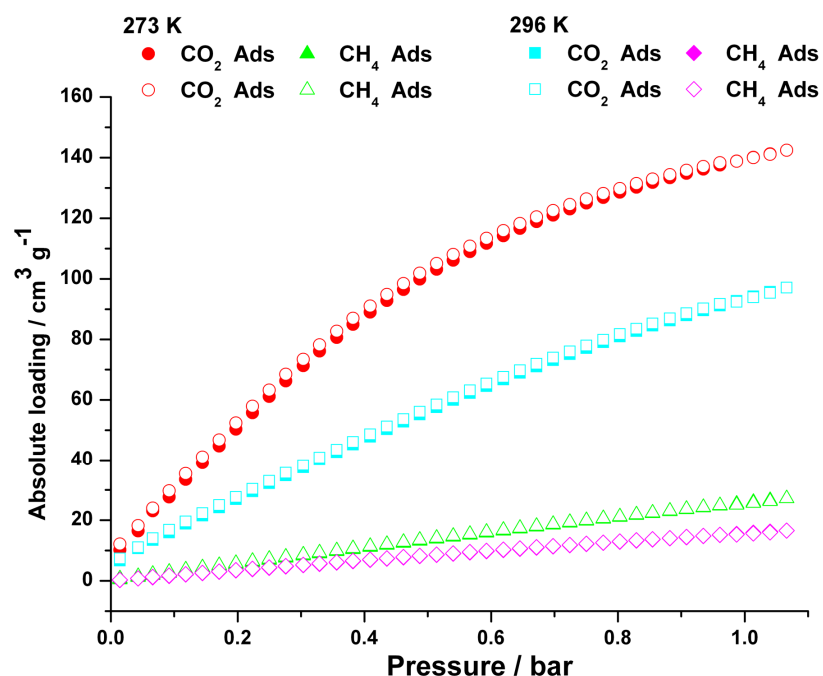


Figure S7. CO_2 and CH_4 adsorption for **InOF-1** at 273 K and 296 K.

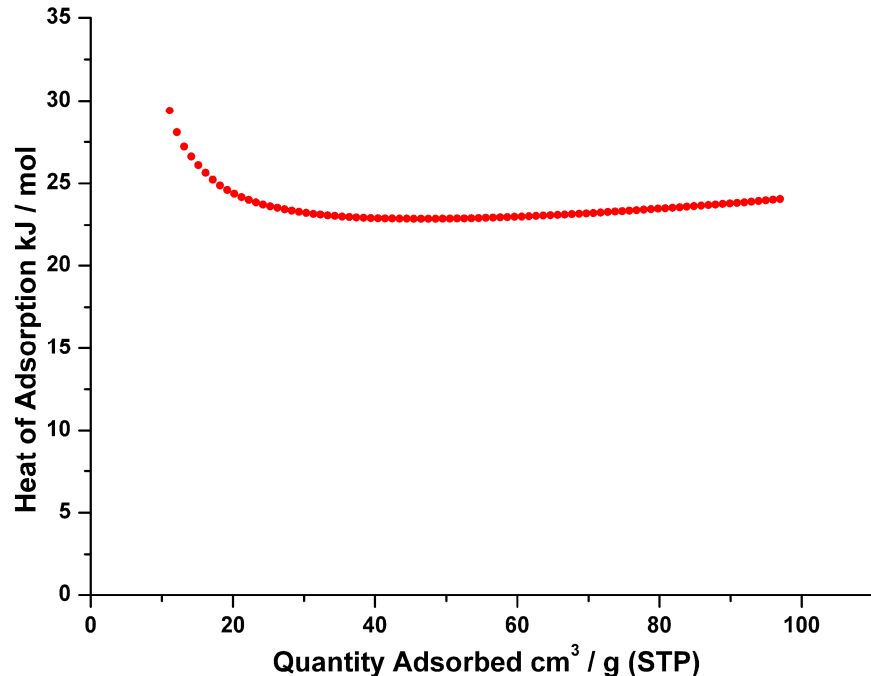


Figure S8. CO₂ heat of adsorption for InOF-1.

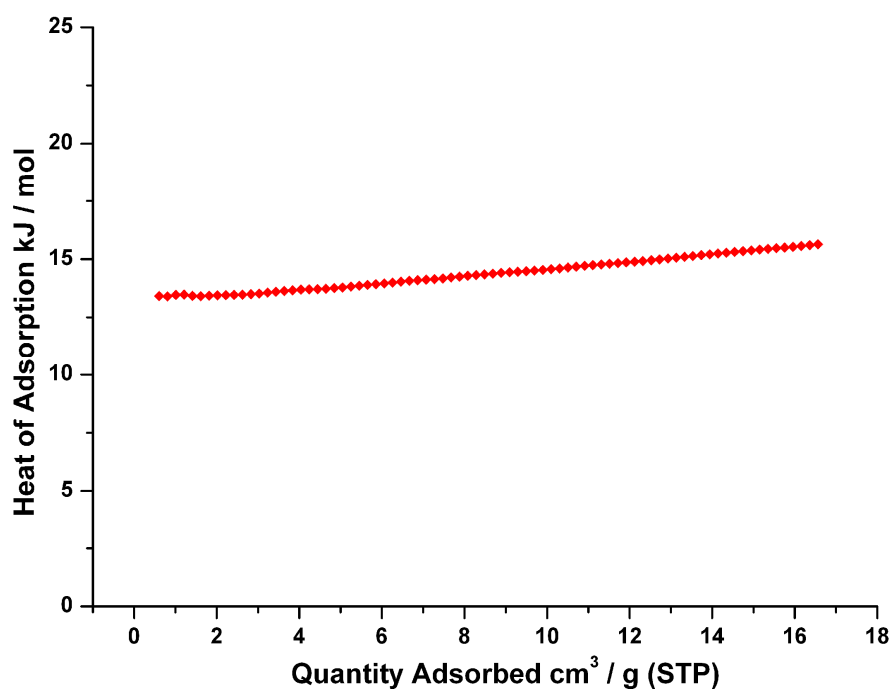


Figure S9. CH₄ heat of adsorption for InOF-1.

6. IAST Selectivity

The written code we used to solve the ideal adsorbed solution theory (IAST) when the adsorption isotherm is fitted by the single-site Langmuir-Freundlich equation:

$$N = A_1 \frac{b_1 P^{c1}}{1 + b_1 P^{c1}}$$

N: molar loading of species i, mmol/g

A: saturation capacity of species i, mmol/g

b: constant, Pa⁻¹

c: constant

The adsorption selectivities, $S_{i/j}$, for binary mixtures of CO₂/CH₄ and CO₂/N₂, defined by

$$S_{i/j} = \frac{q_1/q_2}{p_1/p_2}$$

$S_{i/j}$: adsorption selectivity

q_i : the mole fractions of component in the adsorbed phases

p_i : the mole fractions of component in the bulk phases

The adsorption selectivities were calculated using the Ideal Adsorption Solution Theory (IAST) of Myers and Prausnitz.⁴ The IAST calculations were carried out for equimolar gas-phase mixtures of CO₂ and CH₄, and binary mixture containing 15% CO₂ (y_1) and 85% N₂ (y_2), which is typical of flue gases.

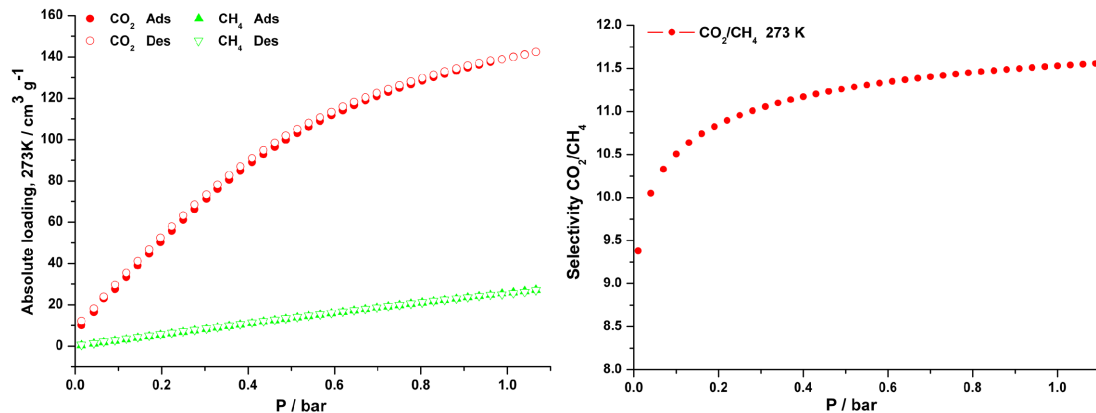


Figure S10. Single component low-pressure gas sorption isotherms for **InOF-1**

toward CO₂ and CH₄, and their selectivity at 273 K.

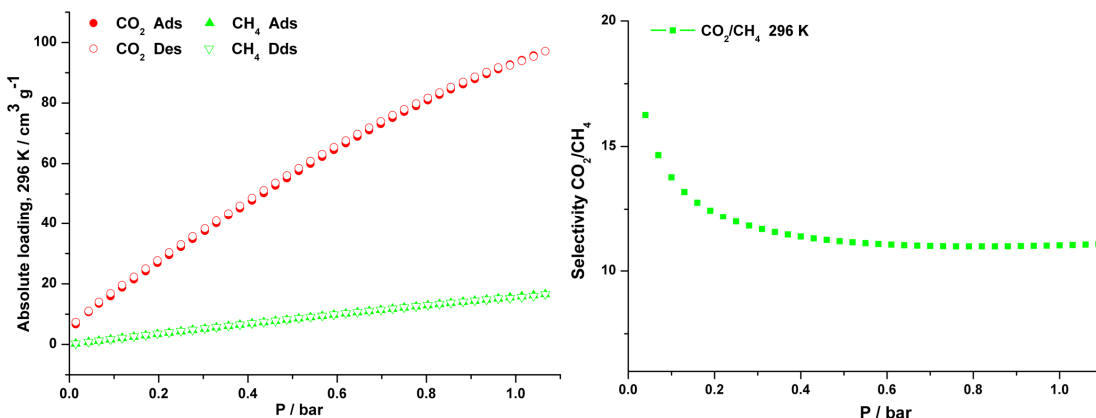


Figure S11. Single component low-pressure gas sorption isotherms for **InOF-1**

toward CO₂ and CH₄, and their selectivity at 296 K.

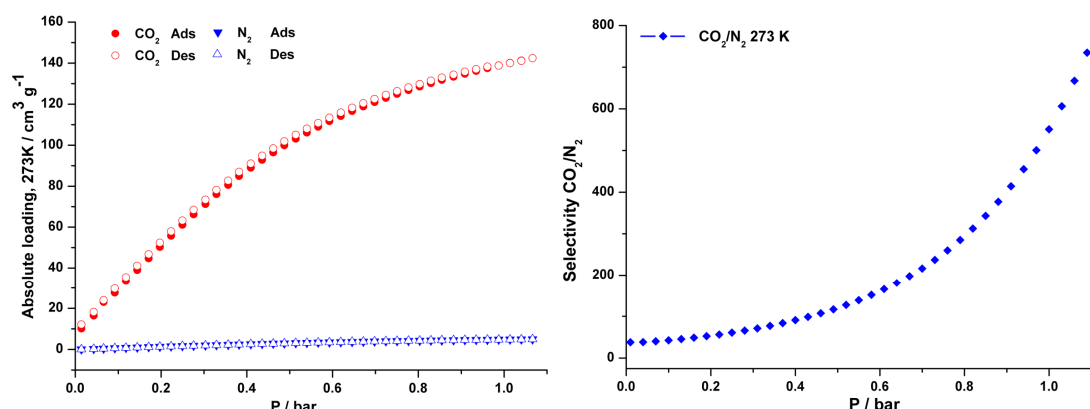


Figure S12. Single component low-pressure gas sorption isotherms for **InOF-1**

toward CO₂ and N₂, and their selectivity at 273 K.

7. Comparisons of CO₂ uptake capacities and selectivities of CO₂ over CH₄

Table S2. CO₂ uptake *vs* BET surface area plotted points for varying MOFs at 273 K.

Compounds	CO ₂ Upatke (mmol/g)	SA _{BET}	Reference
InOF-1	6.26	1065	This work
Cu ₂ (ebtc) ₃	7.95	1828	5
Dy(btc)	6.18	655	6
Cu-EBTC	5.89	1852	7
CAU-1	5.48	1268	8
Zn ₂ (BTetB)	4.48	1370	9
Co ₄ (OH) ₂ (p-CDC) ₃	3.73	1080	10
mmen-Mg ₂ (dobpdc)	6.42	3270	11
PPN-6-CH ₂ DETA	4.3	555	12

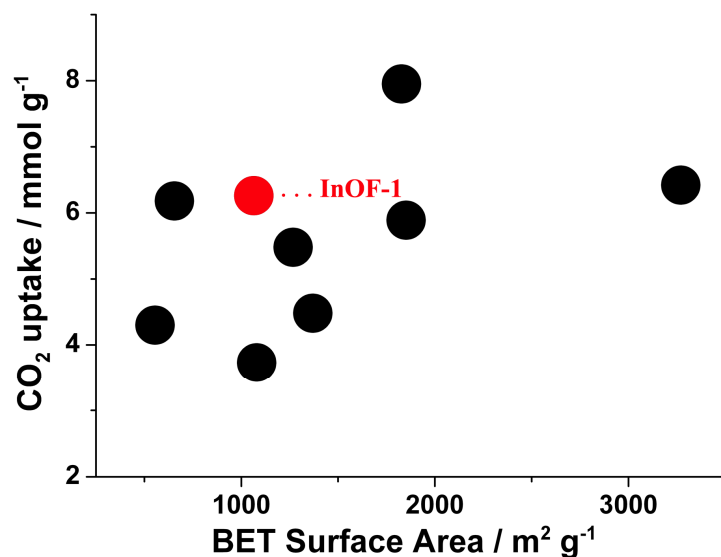


Figure S13. A comparison of BET surface area *versus* CO₂ uptake at 273 K and 1.0 bar.

Table S3. CO₂ uptake *vs* BET surface area plotted points for varying MOFs at 296 K.

Compounds	CO ₂ Upatke (mmol/g)	Selectivity	Reference
MOF-5	2.1	2.3	13
HKUST-1	6.1	6.5	13
Mg-MOF-74	6.25	11.5	13
Zn-MOF-74	4	13	13
Cu(bpy) ₂ (SiF ₆)	5.25	10.5	14
Cu(bpe) ₂ (SiF ₆)	2.75	8.3	14
InOF-1	4.21	11.02	This work
ZIF-100	1.7	5.9	15

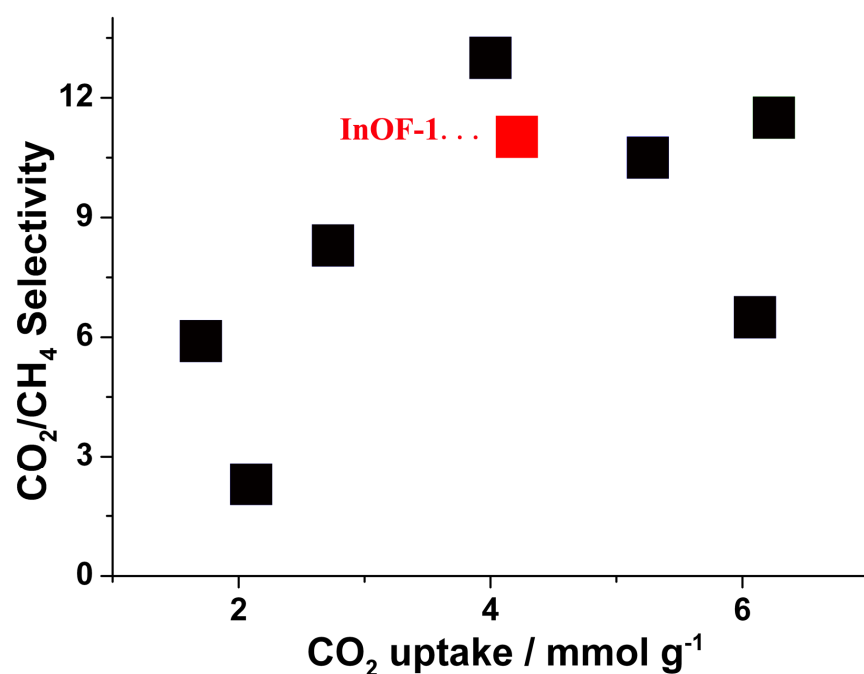


Figure S14. A comparison of CO₂ uptake at 296 K and 1.0 bar *versus* CO₂/CH₄

selectivity based on similar BET surface area.

References.

- [1] Sheldrick, G. M. SHELXS-97, Programs for X-ray Crystal Structure Solution; University of Göttingen: Germany, **1997**.
- [2] (a) A. L. Spek, *J. Appl. Crystallogr.* **2003**, *36*, 7; (b) P. v.d. Sluis and A. L. Spek, *Acta Crystallogr., Sect. A*, **1990**, *46*, 194.
- [3] ASAP 2020 Accelerated Surface Area and Porosimetry System Operator's Manual V4.00, Appendix C, C-43.
- [4] Myers, A. L.; Prausnitz, *J. M. AIChE J.* **1965**, *11*, 121.
- [5] P. Kanoo, K.L. Gurunatha, T.K. Maji, *J. Mater. Chem.* **2010**, *20* (2010) 1322.
- [6] Guo, X.; Zhu, G.; Li, Z.; Sun, F.; Yang, Z.; Qiu, S. *Chem. Commun.* **2006**, 3172.
- [7] Hu, Y.; Xiang, S.; Zhang, W.; Zhang, Z.; Wang, L.; Bai, J.; Chen, B. *Chem. Commun.* **2009**, 7551.
- [8] Si, X.; Jiao, C.; Li, F.; Zhang, J.; Wang, S.; Liu, S.; Li, Z.; Sun, L.; Xu, F.; Gabelica, Z.; Schick, C. *Energy Environ. Sci.* **2011**, *4*, 4522.
- [9] Bae, Y.-S.; Farha, O. K.; Hupp, J. T.; Snurr, R. Q. *J. Mater. Chem.* **2009**, *19*, 2131.
- [10] Farha, O. K.; Spokoyny, A. M.; Mulfort, K. L.; Galli, S.; Hupp, J. T.; Mirkin, C. *A. Small.* **2009**, *15*, 1727.
- [11] McDonald, T. M.; Lee, W. R.; Mason, J. A.; Wiers, B. M.; Hong, C. S.; Long, J. R., *J. Am. Chem. Soc.* **2012**, *134*, 7056-7065.
- [12] Lu, W.; Sculley, J. P.; Yuan, D.; Krishna, R.; Wei, Z.; Zhou, H. C., *Angewandte Chemie*, **2012**, *51*, 7480-7484.

- [13] Simmons, J. M.; Wu, H.; Zhou, W.; Yildirim, T. *Energy & Environmental Science* **2011**, *4*, 2177.
- [14] Burd, S. D.; Ma, S.; Perman, J. A.; Sikora, B. J.; Snurr, R. Q.; Thallapally, P. K.; Tian, J.; Wojtas, L.; Zaworotko, M. J., *J. Am. Chem. Soc.* **2012**, *134*, 3663-3666.
- [15] Wang, B.; Cote, A. P.; Furukawa, H.; O'Keeffe, M.; Yaghi, O. M. *Nature*. **2008**, *453*, 207.